Modeling runoff and soil erosion in the Three-Gorge Reservoir drainage area of China using limited plot data

A-Xing Zhu [a,b], Ping Wang [b], Tongxin Zhu [c,1], Lajiao Chen [d,*], Qiangguo Cai [a], Huiping Liu [e]

[a] State Key Lab of Resources and Environmental Information System, Institute of Geographical Sciences and Natural Resources Research, Chinese Academy of Sciences, Beijing, China
[b] Department of Geography, University of Wisconsin-Madison, Madison, USA
[c] Department of Geography, University of Minnesota-Duluth, Duluth, USA
[d] Institute of Remote Sensing and Digital Earth, Chinese Academy of Sciences, Beijing, China
[e] Department of Geography, Beijing Normal University, Beijing, China

ARTICLE INFO

SUMMARY

This paper presents a modeling approach to simulate runoff and soil erosion at the small watersheds of the Three-Gorge Reservoir drainage area in China by using limited plot data on runoff-soil erosion. The approach coupled the empirical relationships between soil loss and runoff. This relationship is derived from the experimental plots under different land use types with a spatially distributed hydrological model, WetSpa Extension, to calculate soil loss in grid cells. A topographic factor was also developed to account for the impacts of topography on soil loss. Finally, a constant Sediment Delivery Ratio (SDR) was applied to calculate sediment yields transported to the catchment outlet from grid cells. The coupled model was first calibrated for the study areas using the observed continuous discharge data and event-based sediment data over the period from May 1st through October 31st of 2001 in a small sub-catchment in Sichuan, China. The calibrated model was then applied to the same sub-catchment over the same period of every year from 1993 to 2000 as well as the neighboring catchments to assess the performance and stability of the model. A comparison of observed and simulated stream flows indicates that the model performance was acceptable in six (1993, 1994, 1996, 1998, 1999 and 2000) of the 8 years with Nash–Sutcliffe Efficiency (NSE) of 0.654 and 0.729 for weekly and monthly flow discharges, respectively. A comparison between the observed and simulated sediment yields showed that the simulation of sediment yields was very satisfactory (NSE = 0.88) and the spatial variability of soil erosion rates within the catchments was predominantly controlled by land use types. Finally, the model was applied to assess the efficacy of soil conservation through land use changes in Sub-catchment No. 2. The results clearly indicated that land use changes after 1990s have been very effective in reducing both runoff and sediment. This study suggests that experimental plot data is an effective supplement to modeling spatial variation of soil erosion, albeit their various limitations.

© 2013 Elsevier B.V. All rights reserved.

1. Introduction

Soil erosion remains one of the world's biggest environmental problems, threatening both developed and developing countries (ISCO, 2002). Erosion by water not only strips the fertile topsoil on site, but also degrades water quality and clogs streams, rivers, and reservoirs with transported sediments off site. Sedimentation in reservoirs has become an increasing concern around the world. MahMood (1987) estimated that around 50 km^3 of sediment – or 1% of global reservoir storage capacity – is trapped behind the

world's dams every year. Large reservoirs in the US lose storage capacity at an average rate of around 0.2% per year whereas major reservoirs in China lose capacity at an annual rate of 2.3% (McCully, 1996). As an extreme example, the reservoir behind the SanMenXia Dam constructed on the Yellow River of China in 1960 lost 40 percent of the initial storage capacity in the first 4 years due to the massive load of sediments eroded from the Loess Plateau. The Three-Gorge Reservoir (TGR), formed behind the Three-Gorge Dam (TGD) on the Yangtzi River, is over 600 km long and more than 1000 km^2 of water area. It is estimated that TGR trapped about 162 million tons of sediment annually in 2003–2007 after the Three-Gorge Dam (TGD), the world's largest hydro dam, began to operate in 2003,which represents 84% of sediment discharge in the pre-TGD period (1986–2002) (Hu et al., 2009). Sedimentation in the reservoir behind the TGD results in a progressive reduction of the storage capacity and triggers a series of physical, chemical

* Corresponding author. Address: Institute of Remote Sensing and Digital Earth, Chinese Academy of Sciences, Beijing 100094, China. Tel.: +86 010 82178973.
   E-mail address: chenlajiao@ceode.ac.cn (L. Chen).
[1] Address: Department of Geography, University of Minnesota-Duluth, 329A Cina, 1123 University Dr., Duluth, MN 55812, USA. Tel.: +1 218 726 8480; fax: +1 218 726 6540.
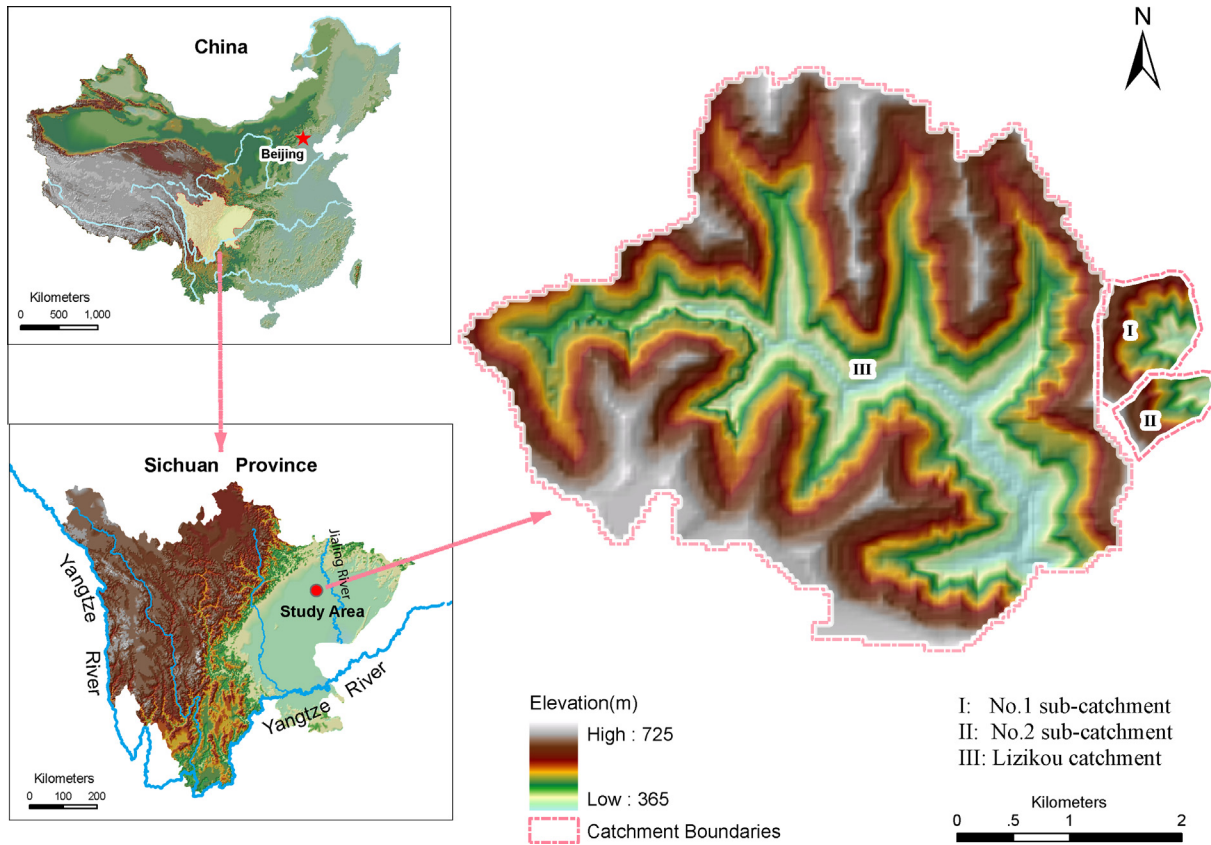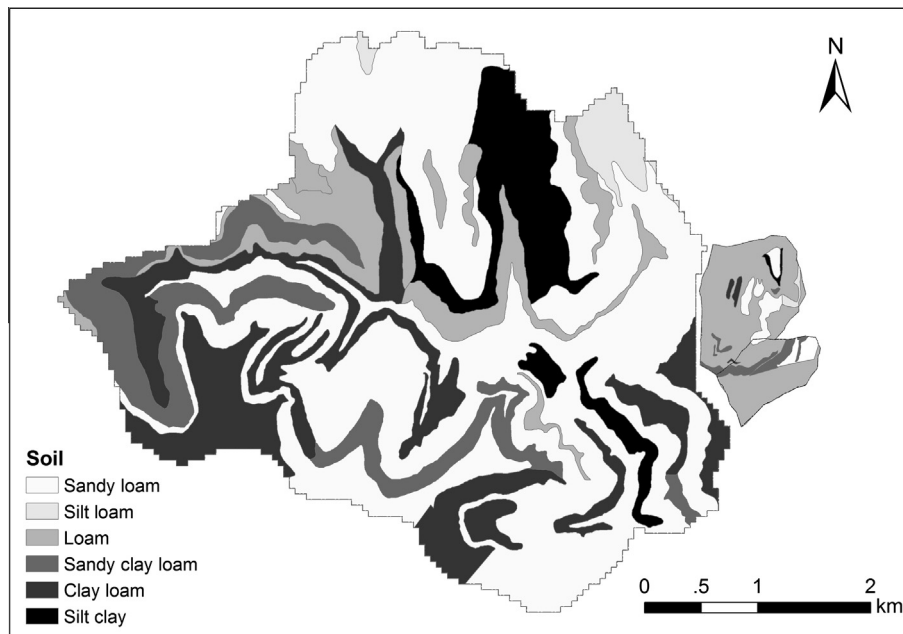
Fig. 1. Map and DEM of study area.

Fig. 2. Soils in HeMingGuan and LiZiKou catchments.

and ecological impact on the environment (Lu and Higgitt, 2000). The fundamental solution to sedimentation is to reduce sediments transported into the reservoir. The TGR has a drainage area of about 1 million km². Integrated small watershed management (ISWM) that aims to control soil erosion through implementing comprehensive measures (e.g. changing inappropriate land use, terracing slope lands, planting trees and grasses) has developed rapidly in the area since the 1990s. The ISWM has been conducted in more than 5000 small watersheds with an area of 96,000 km² (Shi et al., 2012; Liao, 2010). The small watersheds refer to those
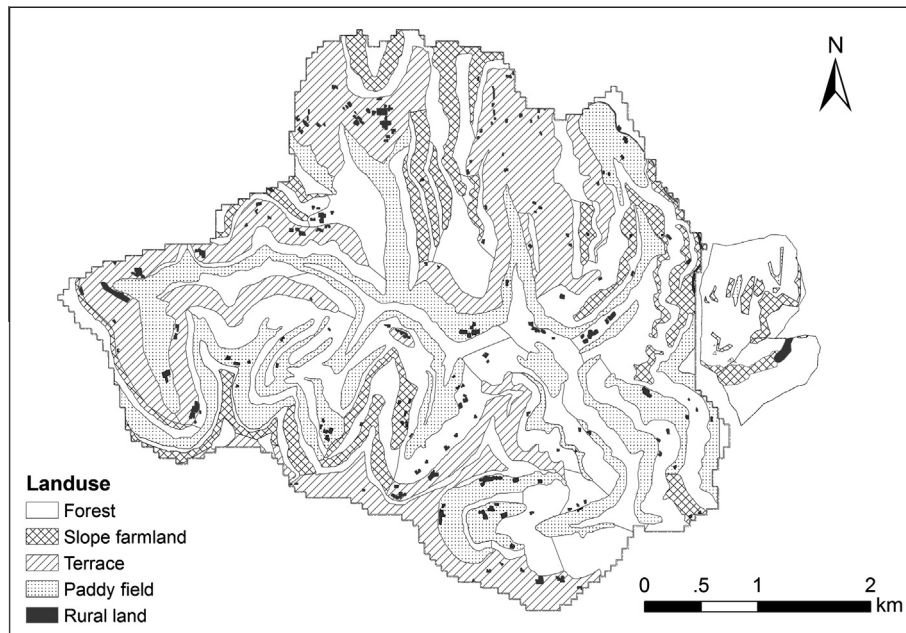
Fig. 3. Land uses in HeMingGuan and LiZiKou catchments.

Table 1
Soils of the study area.

Soil texture	Area (km²)	Percentage (%)
LiZikou catchment		
Sandy loam	9.93	50.7
Silt loam	4.42	2.3
Loam	1.98	10.1
Sandy clay loam	2.01	10.3
Clay loam	3.47	17.7
Silt clay	1.74	8.9
Sub-catchment No. 1		
Sandy loam	0.1022	12.7
Silt loam	0.0182	2.3
Loam	0.6284	78.3
Sandy clay loam	0.0199	2.5
Clay loam	0.0193	2.4
Silt clay	0.0145	1.8
Sub-catchment No. 2		
Sandy loam	0.0501	11.9
Loam	0.3013	71.7
Sandy clay loam	0.0682	16.2
Clay loam	0.0006	0.2

Table 2
Landuse of the study area.

Landuse type	Area (km²)	Percentage (%)
LiZiKou catchment		
Forest	7.85	50.7
Slope farmland	2.00	2.3
Terrace	5.32	10.1
Paddy field	4.12	10.3
Rural land	0.26	17.7
Sub-catchment No. 1		
Slope farmland	0.128	16.1
Terrace	0.023	2.9
Forest	0.649	81.0
Sub-catchment No. 2		
Forest	0.327	78.4
Slope farmland	0.071	17.2
Paddy field	0.0001	0.0
Rural land	0.018	4.4

with a typical size of 20 km² or less. The purpose of this study is to assess soil and water loss as well as the efficacy of conservation practices in the reservoir drainage area using a newly developed semi-empirical distributed erosion model.

A considerable number of models have been developed to simulate soil erosion processes and to assess the impact of land use changes and the efficacy of soil conservation practices (e.g. SWAT, Arnold et al., 1998; HEC, 1995). Physically based erosion models such as WEPP (Nearing et al., 1989), LISEM (De Roo et al., 1996), and EUROSEM (Morgan et al., 1998) always require an overwhelming number of parameters to characterize catchments and to describe erosion processes. The majority of the watersheds in developing countries do not have sufficient measurements to meet the parameter requirements of these models. In contrast, empirical models usually have a lower parameter requirement than physically based models. USLE (Wischmeier and Smith, 1978) and its modified versions such as MUSLE (Williams, 1975) and RUSLE (Renard et al., 1997) are the most typical and widely used empirical models. USLE and its revised versions were developed based on data collected from numerous experimental plots in the US. When applied to areas where environmental conditions and farming techniques as well as soil conservation practices significantly divert from the U.S., variables in USLE series need to be modified to accommodate local characteristics (e.g., Lu and Higgitt, 2001; Hoyos, 2005; Zhang et al., 2008; Liu et al., 1994, 2000). The cropping and land preparation in China are completely different from the US (Shi et al., 2012). The farming lands in the mountainous TGR drainage area are typically very small in size (less than 1 acre) and irregular in shape, and ploughed by animals instead of tractors. The field borders between small land parcels owned by different households are varied, i.e. raised earth banks, small ditches, and vegetative filter strips, etc. All of those features ensure the needs for the modifications of the USLE parameter values, which would require statistical analysis on a large collection of data with long series of observations on comprehensively designed experimental plots.

The issue of input data as a major barrier to model applications to the TGR drainage area is even further complicated by a mismatch between existing data and the data required by the models. Over the past decades, a considerable number of experimental

Table 3
Data list collected in HMG and LZK catchments.

	Digital maps	Precipitation (daily)	PET (daily)	Discharge (daily)	Sediment (storm events)
Experimental Plots	/	/	/	1983–2001 (storm events)	1983–2001
HeMingGuan No.2	DEM; Land use map; soil map	1986–1988, 1994, 1996, 1998–2001	1986–1988, 1994, 1996, 1998–2001	1986–1988, 1994, 1996, 1998–2001	1986–1988, 1994, 1996, 1998–2000
HeMingGuan No.1	DEM; Land use map; soil map	1994–1996	/[*]	1994–1996	1994–1996
LiZiKou	DEM; Land use map; soil map	2004–2005	/[*]	2004–2005	2004–2005

[*] PET data of No.1 sub-catchment and LZK catchment was unavailable, we used that of No.2 sub-catchment instead.

watersheds have been set up to study soil erosion and its counter-measures in the region. In a "typical" field setting, sediment and water discharges were measured from a limited number of erosion plots under different land use types and conservation practices. As originally collected not for the purpose of model applications, the data could not be used as input to the existing erosion models. Accordingly, in this study, we will develop a modeling approach to simulating runoff and soil erosion rates at grid cell level, and stream flow and sediment yield at catchment outlet based on the existing data collected under a "typical" field setting in the region. The simulation at grid cell level enables to evaluate the spatial variability of soil erosion and runoff generation within the watershed and to assess the efficacy of different scenarios of land use changes/conservation practices in reducing soil and water loss. The computation of sediment yields at catchment outlet is the key to estimating sediment input to the reservoir. We will also examine the problems associated with the modeling approach and their causes, which justifies future improvements aimed at widely applying the model in the TGR drainage area.

2. Physical settings

The study catchments, HeMingGuan and LiZiKou, are located in the drainage area of the JiaLingJiang River, one of the four main tributaries of the upper Yangtze River (Fig. 1). HeMingGuan is an experimental catchment for soil and water conservation research, with a drainage area of 1.2 km². Flow discharge and sediment yield data were collected at the outlets of two sub-catchments, referred to as Sub-catchment No. 1 and Sub-catchment No. 2 with 0.8 km² and 0.4 km² in size, respectively. LiZikou catchment has an area of 19.6 km². Both HeMingGuan and LiZiKou catchments have similar physical characteristics, with elevations ranging from 365 m to 725 m and a mean slope gradient of 19%. Digital Elevation Model (DEM) for HeMingGuan catchment has a resolution of 10 m and was derived from a contour map at scale of 1:10,000 with a 5 m contour interval. Due to data availability the DEM for LiZiKou catchment has a resolution of 50 m. It should be noted that the difference in DEM resolution between the catchments may contribute the errors in model simulations. Soil map (Fig. 2) and land use map (Fig. 3) were created from field survey maps at 1:10,000 scale. To match with the DEM resolutions, the soil map and the landuse maps were rasterized with a grid cell size of 10 m and 50 m for HeMingGuan and LiZiKou, respectively. Soils over the study areas include sandy loam, silt loam, loam, sandy clay loam, clay loam and silt clay soil, with predominance of loamy (>70%) in HeMing-Guan, and sandy loamy and clay loamy (68.4%) in LiZiKou (Table 1). To counter against serious erosion in the areas a set of soil conservation practices via land use changes was put in place from late 1980s to early 1990s. Land use types were mainly crop lands (tillage) and un-cultivated grass lands prior to the implementation of conservation practices, and have been dominated by planted forest

lands (80%) in HeMingGuan, and croplands (48.5%) as well as forest lands (41%) in LiZiKou after 1990 (Fig. 3 and Table 2).

Three experimental plots were set up in Sub-catchment No. 2 of HeMingGuan in 1983. Runoff generated from individual storms was collected by a container at the lower end of each plot. Samples were taken at the end of each storm from the container and the sediment concentrations of the samples were then determined in the lab. In sum, total water discharge and sediment yield were measured for individual storm events from 1983 to 2001. The collected data of the plots are listed in Table 3. All the plots have similar size, slope gradient, slope length and soil type (sandy loam, the major soil in the catchment). The only major difference among them is their land use types. The experiments were conducted on the plots in two phases. From the first phase (1983–1986) to the second phase (1987–2001), land use on Plot No. 1 was changed from unmanaged land with sparse natural vegetation (broadleaf trees and shrubs) to wood land through tree planting; land use on Plot No. 2 was changed from uncultivated land with sparse grasses to grass land through grass planting; land use on Plot No. 3 was changed from tillage (crop land) to terrace. Therefore, the data collected on the three plots during the two phases can be used to analyze the relationship between water discharge and sediment yield under the landuse conditions of uncultivated land, wood land, grass land, tillage (crop land), and terrace, which represent all the main land use types in the study area.

3. Model description

A coupled modeling approach was taken in the study. The approach consists of three major parts: (1) Simulation of hydrological processes using a physically-based and spatially-distributed hydrological model, WetSpa Extension (Liu, 1999; Liu et al., 2002, 2003; Liu and De Smedt, 2004); (2) Simulation of soil loss in grid cells using the empirical relationships between soil loss and runoff derived from the experimental plots under different land use types and the runoff from WetSap Extension; (3) Estimation of sediment yield at catchment outlet.

3.1. Simulation of hydrological processes

WetSpa Extension was employed to simulate hydrological processes (i.e., overland flow rates, soil moisture etc.), and to estimate the volume of surface runoff that was later used to calculate soil loss at grid level. WetSpa is a process-based, spatially-distributed hydrological model for predicting the Water and Energy Transfer between Soil, Plants and Atmosphere on regional or basin scale and daily time step, and was originally developed in the Vrije Universiteit Brussel, Belgium (Wang et al., 1997; Batelaan et al., 1996). WetSpa Extension, a modified version of WetSpa, is a GIS-based hydrological model for flood prediction and water balance simulation at catchment scale, and is capable of predicting outflow hydrograph at basin outlet or any converging point in a watershed
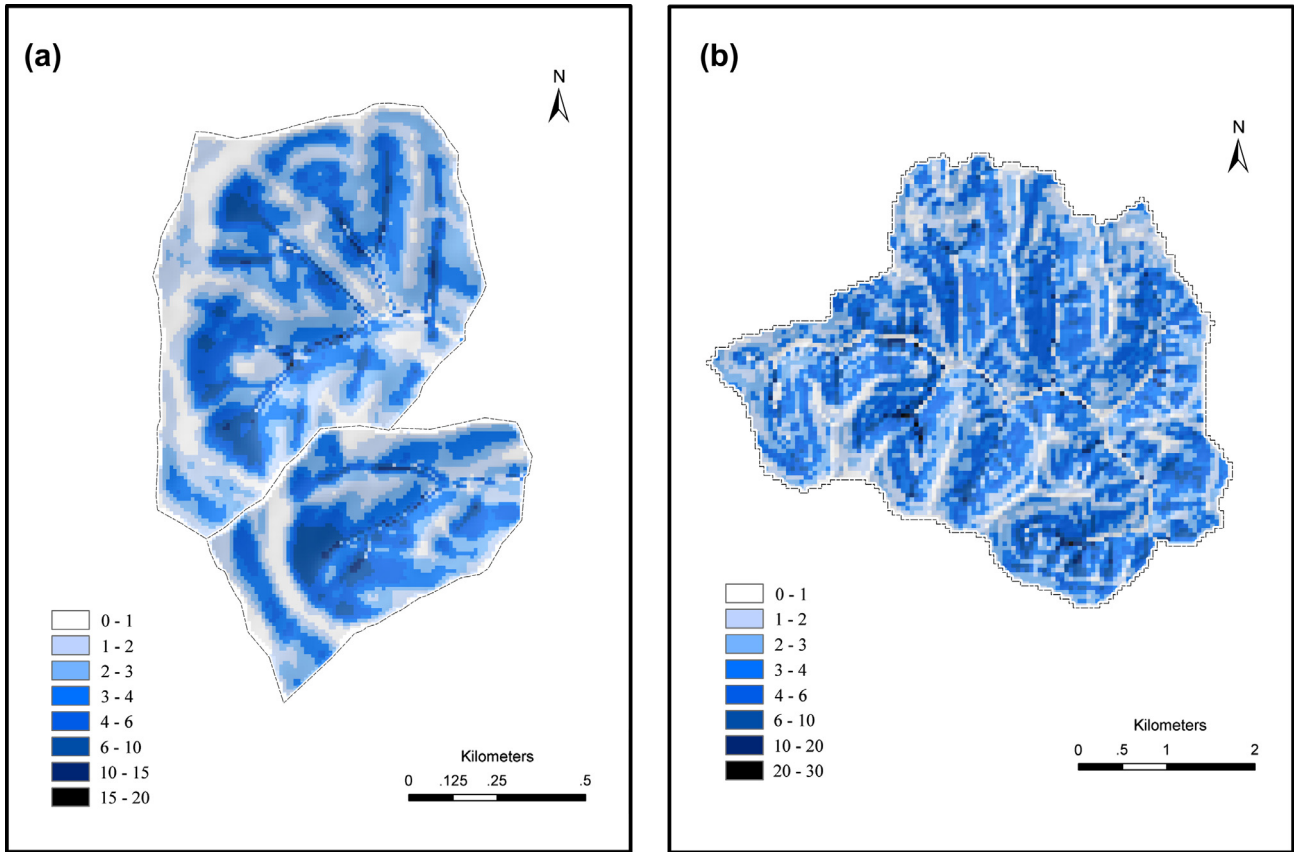
Fig. 4. Distribution of the topographic factor in the study areas (a) Subcatchment Nos. 1 and 2; (b) LiZiKou catchment.

with a variable time step (Liu, 1999; Liu et al., 2002, 2003; Liu and De Smedt, 2004; De Smedt et al., 2000; Liu and De Smedt, 2004). The model conceptualizes a basin hydrological system being composed of atmosphere, canopy, root zone, transmission zone and saturation zone. The basin is divided into a number of grid cells in order to deal with the heterogeneity. Each cell is further divided into a bare soil and vegetated part, for which the water and energy balance are maintained (Liu and De Smedt, 2004). The model programs were developed using ArcView Avenue and Fortran language and the WetSpa Extension can be run on a personal desk computer.

In WetSpa Extension, each grid cell is divided into four layers in the vertical direction: canopy, root zone, transmission zone, and saturated zone. The simulated hydrologic processes are canopy interception, depression storage, surface runoff, infiltration, evapotranspiration, percolation, interflow, groundwater recharge, and water balance in root zone and saturated zone. Total discharge consists of surface runoff, interflow and groundwater discharge, and its routing is conducted by an approximate solution to the diffusive wave equation in the form of a density function of the first passage time distribution (Liu et al., 2003). With DEM, land use map, soil map and data on precipitation, potential evapotranspiration (PET),
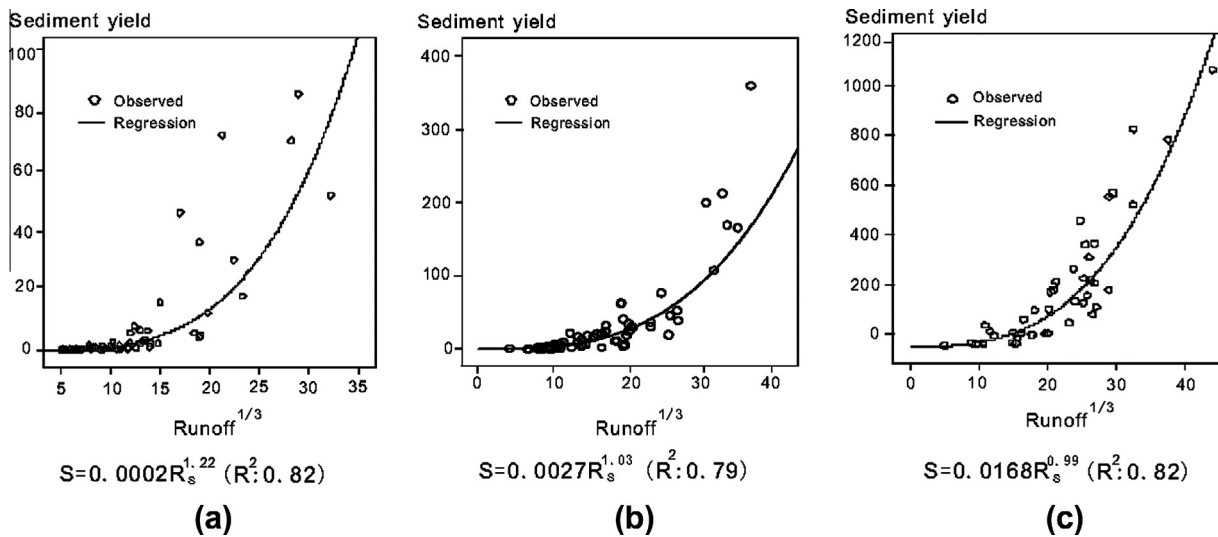

$$S = 0.0002R_s^{1.22} \quad (R_s^2 : 0.82)$$

(a)

$$S = 0.0027R_s^{1.03} \quad (R_s^2 : 0.79)$$

(b)

$$S = 0.0168R_s^{0.99} \quad (R_s^2 : 0.82)$$

(c)

Fig. 5. Regression functions describing relationship of sediment yield and surface runoff under the land use type of (a) planted wool land, (b) terrace land, and (c) crop land.

temperature as inputs, the model can predict hydrographs for any location in the channel network, and simulate spatially-distributed hydrological variables, including surface runoff, which can be used to simulate soil loss in each grid cell.

In this model, surface runoff is calculated using a modified rational method (Liu and De Smedt, 2004):

$$R_s = C_p P_n (SW/SW_s)^{\alpha} \tag{1}$$

where R_s is the rate of surface runoff (mm), C_p is a potential runoff coefficient, depending on slope, soil type and land use combinations, P_n is the rainfall intensity after canopy interception (mm/h), SW and SW_s are actual and saturated soil moisture content respectively (m³/m³), and α is an empirical exponent. In general, the equation accounts for the effect of slope, soil type, land use, soil moisture, rainfall intensity and its duration on the production of surface runoff in a realistic way. Soil moisture is also simulated for the root zone in each grid at the beginning and the end of each time step based on the following water equation (Liu and De Smedt, 2004).

$$D_i[\theta_i(t) - \theta_i(t-1)] = F_i(t) - ES_i(t) - RG_i(t) - RI_i(t) \tag{2}$$

in which $\theta_i(t)$ and $\theta_i(t-1)$ are cell soil moisture content at time step t and $t-1$ (m³/m³), Di is the root depth (mm); $F_i(t)$ is the infiltration through soil surface for the time increment (mm), including the infiltration during the rainstorm and the infiltration from depression storage after the rainstorm (mm), $ES_i(t)$ is the actual evapotranspiration from the soil for the time increment (mm), $RG_i(t)$ is the percolation out of root zone or groundwater recharge (mm), and $RI_i(t)$ is the interflow or lateral shallow subsurface flow out of the cell.

3.2. Simulation of soil erosion in grid cells

In a small watershed, we assume rainfall is spatially uniform and the major factors affecting erosion variability are land use/soil conservation practices, topographic conditions and soil properties.

First of all, the relation between runoff and erosion was derived from the field data collected on the erosion plots with different land uses but same topographic and soil conditions (Fig. 5). We then use the empirical functions drawn from the plot data as the basis for calculating soil loss for each grid cell of different topographic and soil attributes. Most of the soils in the study area are loamy soils with small difference and the spatial variation in soil attributes over the study areas is much related to topography and vegetation types (land use) (Figs. 2 and 3). Accordingly, the relationship between runoff and soil loss over the area largely depends on the topography and land use. However, for areas with complicated soil patterns (due to geology or other factors) a separate soil variable needs to be included in the model.

There have been continuous efforts in integrating topography into simulating watershed processes and deriving it from DEM (i.e., Band, 1986, 1993; Moore and Burch, 1986a; Band et al., 2011). In this study, in order to consider the effect of topography on soil erosion, we adopt a physically-based function developed by Moore and Burch (1986b). Based on unit stream power theory, the relationship between soil loss in a field and the topographic variables is expressed as:

$$E \propto \left[\left(\frac{A_{in}}{w} \right)^{0.4} \cdot \sin^{1.3} \theta \right]^{\beta} \tag{3}$$

where A_{in} is the upslope contributing area to the field (m²/m); w is the length of contour in the field (m); θ is slope gradient of the field (°); β, based on Moore and Burch (1986b), is a function of physical variables including particle size of sediment, velocity, etc., and is set to 1 in this case because our watersheds are among those suggested by Moore and Burch (1986a) to take the value of 1. In this equation, the contributing area on unit contour length (A_{in}/w) in a watershed is equivalent to slope length in a hillslope in terms of their impact
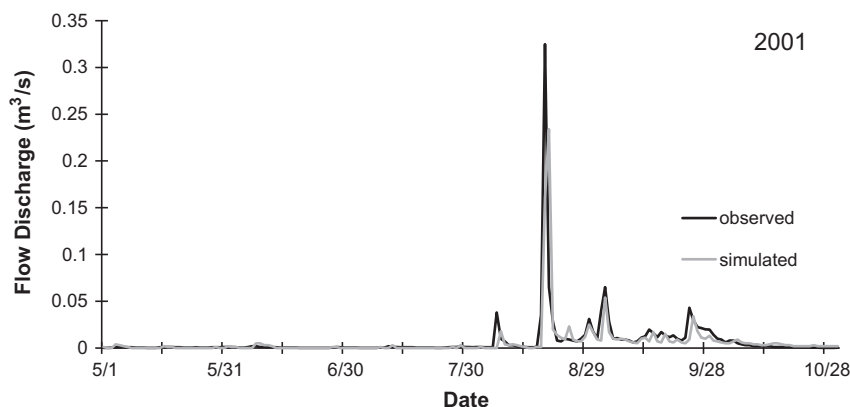
Table 4
Input parameters to the conceptual soil erosion model for Lizikou watershed.

Soil parameters	Sandy loam	Silt loam	Loam	Sandy clay loam	Clay loam	Silt clay
Saturated hydraulic conductivity (mm/h)	25.92	13.32	5.58	4.32	1.51	0.9
Porosity (m³/m³)	0.453	0.501	0.463	0.398	0.464	0.479
Field capacity (m³/m³)	0.19	0.284	0.232	0.244	0.31	0.371
Wilting point (m³/m³)	0.085	0.135	0.116	0.136	0.187	0.251
Residual moisture (m³/m³)	0.041	0.015	0.027	0.068	0.075	0.056
Pore size distribution index (–)	4.5	4.98	5.77	7.2	8.32	10.38

Vegetation parameters	Slope farmland/ terrace/paddy field		Forest	Impervious area
Vegetated fraction (%)	80		80	0
Leaf area index (–)	0.5–0.6		1.0–6.0	0.0–0.0
Root depth (m)	1		2	0
Manning's coefficient (m^{-1/3}s)	0.15		0.8	0.02
Interception capacity (mm)	0.05–1.00		0.15–2.00	0.00–0.00

Erosion parameters	Slope farmland	Terrace	Forest
Coefficient of runoff and erosion relationship	0.0168	0.0003	0.0002

Fig. 6. Observed and calibrated hydrographs over the period of May 1st through October 31st, 2001 in Sub-catchment No. 2.
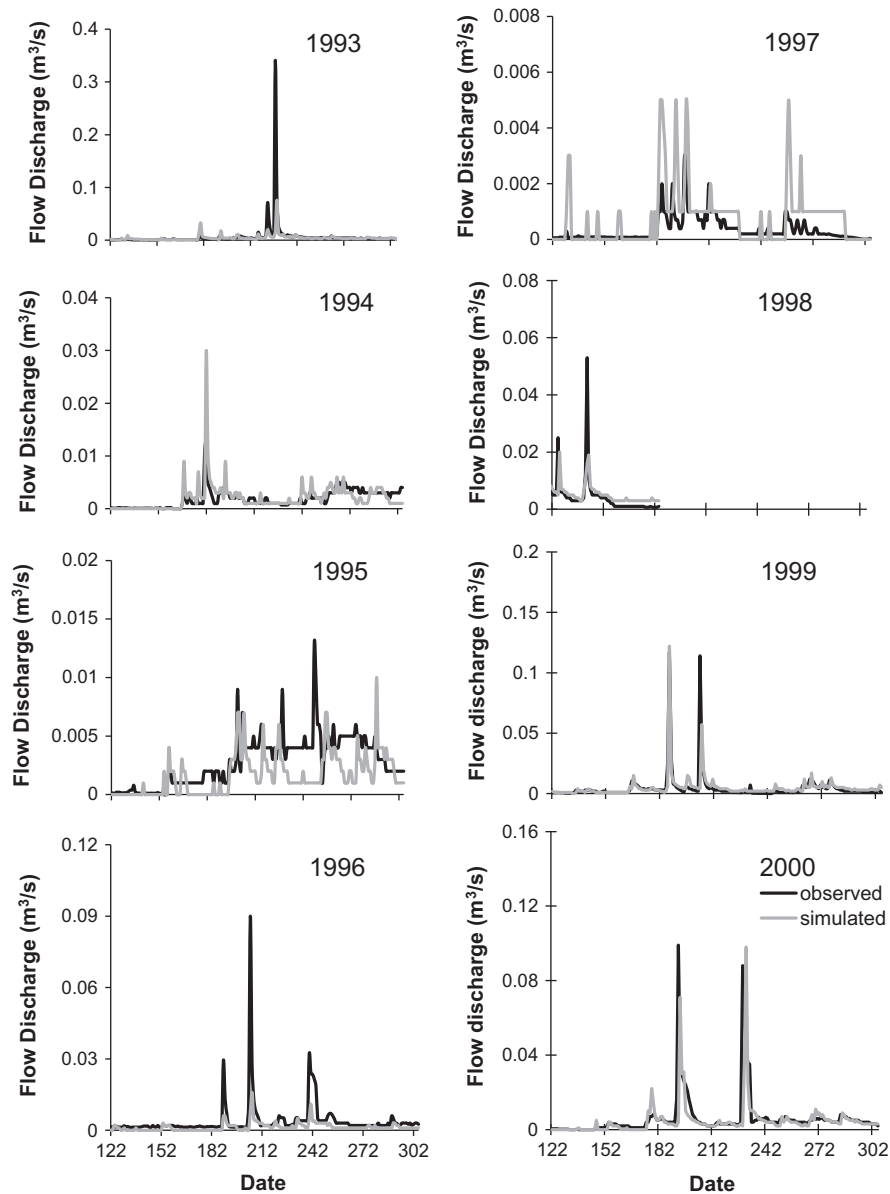
Fig. 7. Observed and simulated streamflow hydrographs for each year from 1993 to 2000 in Sub-catchment No. 2.

Table 5
Model performance of streamflow discharge simulation in the year 1993 through 2001 in the Sub-catchment No. 2.

Year	NSE	PBIAS	RSR	R^2
1993	0.128	0.307	0.871	0.392
1994	0.470	0.057	0.529	0.717
1995	−0.210	0.404	1.210	0.459
1996	0.142	0.649	0.857	0.640
1997	−3.950	−1.121	4.950	0.788
1998	0.437	−0.025	0.562	0.662
1999	0.500	−0.094	0.499	0.714
2000	0.100	−0.002	0.899	0.478

Table 6
Model performance of peakflow, daily, weekly and monthly discharge simulation.

	N.S.E	RSR	PBIAS	R^2
Peak flow discharge	0.27	0.854	0.448	0.437
Daily discharge	0.029	0.942	0.081	0.715
Weekly discharge	0.654	0.119	0.069	0.817
Monthly discharge	0.729	0.520	0.127	0.877

on soil erosion (Kirkby and Chorley, 1967; Carson and Kirkby, 1972; Moore and Nieber, 1989). According to Eq. (3), the topographic factor can be introduced as a ratio to account for differences in soil loss between experimental plots and grid cells in watershed caused by differences in topographic features. Considering β is 1 in our case,

the topographic factor in a field in the catchment can be expressed as:

$$T = \left(\frac{SL}{SL_0}\right)^{0.4} \left(\frac{\sin\theta}{\sin\theta_0}\right)^{1.3} \tag{4}$$

where SL is the slope length of the field (m), equivalent to A_{in}/w in Eq. (3); SL_0 is the slope length of the plot (m); θ is the slope gradient of the field (°), and θ_0 is the slope gradient of the plot (°). It should be noted that the slope length factor has been referred to in the

context of a complete landscape unit (hillslope, catchment, or watershed). When applied to grid cells, the slope length factor needs to be modified for a discrete slope segment which is the role of a grid cell to a catchment. A method that automatically calculates slope length factor in grid cells based on DEM developed by Desmet and Govers (1996) was adopted in our study. Based on the algorithm of calculating slope length factor for slope segments proposed by Foster and Wischmeier (1974), the slope length factor for a grid cell is computed by the following equation (Desmet and Govers, 1996):

$$L_i = \frac{(A_{i-in} + D^2)^{m+1} - A_{i-in}^{m+1}}{D^{m+2} \chi_i^m SL_0^m} \tag{5}$$

where L_i represents the slope length factor for grid cell i (m), A_{i-in} is the contributing area for grid cell i (m^2), D is the grid cell size (m), x_i is a weight coefficient, calculated by $sin\ a_i + cos\ a_i$ (a_i is the slope aspect in grid cell i, $D \cdot x_i$ means effective contour length in grid cell i); and m is the exponent of slope length that the soil loss is proportional to. By replacing the slope length factor $(SL/SL_0)^{0.4}$ in Eq. (4) with Eq. (5) (m equals to 0.4 in this case), the topographic factor for a grid cell in our research is calculated by the following equation:

$$T_i = \frac{(A_{i-in} + D^2)^{1.4} - A_{i-in}^{1.4}}{D^{2.4} \chi_i^{0.4} L_{0-k}^{0.4}} \cdot \left(\frac{\sin \theta_i}{\sin \theta_{0-k}} \right)^{1.3} \tag{6}$$

where L_{0-k} is the slope length (m) for the corresponding experimental plot that has the same land use with grid cell i; θ_i and θ_0 is slope gradient (°) for grid cell i and the corresponding plot, respectively. The contributing area A_{i-in} (m^2) here is calculated using multi-flow direction algorithm MFD-md proposed by Qin et al. (2007), which is more probable compared to other multi-flow direction algorithms. With Eq. (6), the distribution of topographic factor in the study areas was computed based on DEM. The result is shown in Fig. 4a and b. The topographic factor represents the combined influence of local slope and relative position of a grid cell in the drainage system on the local soil loss. The values of T factor in the ridge and valley areas are generally small because the slope gradients are low and erosion is less likely to happen in these flat areas. Values of T factor are generally large in the middle part of slopes where is more prone to erosion. The largest values of T factor appear at grid cells along the stream line, the non-flat areas with high flow accumulation. Finally, soil loss for grid cells can be calculated by the following equation:

$$SY_i = f_k(R_{si}) \cdot T_i \tag{7}$$

where SY_i is soil loss in grid cell i (kg/m^2); R_{si} is surface runoff in grid cell i calculated by WetSpa Extension; f_k is empirical function expressing the relationship between surface runoff and soil loss under land use k derived from the limited plot data (see Section 4); and T_i is the topographic factor in grid cell i, which is derived from Eq. (6).

3.3. Estimation of sediment yield at catchment outlet

Eroded sediment can be deposited or be re-suspended during the process of transport from overland (grid cells) to outlets of catchments. Simulation of sediment transport and deposition processes is complicated and requires a number of input parameters (Morgan et al., 1998), which will limit the application of the model and therefore derail the purpose of this study. Besides, sediment transport interrupted by variable types of field borders between small land parcels owned by different households in the catchment are extremely difficult to be characterized in a process-based transport-deposition model. The sediment delivery ratio (SDR) is a simple way to account for transport of sediment. In this study,

Table 7
A comparison of the simulated and observed erosion in No. 1 Sub-catchment and Lizikou catchment.

Catchment	Events	Measured erosion (tons)	Simulated erosion (tons)
No.1 Subcatchment	1	8.416	8.7081
	2	0.667	0.9732
	3	8.11	5.777
	4	1.834	1.736
	5	1.237	2.695
	6	1.723	1.764
	7	0.264	0.743
	8	0.833	3.007
	9	2.189	3.570
	10	18.336	7.379
Lizikou catchment	11	13.382	28.753
	12	86.027	92.852
	13	58.915	42.231
	14	28.616	40.594
	15	21.907	48.247
	16	81.755	83.250

the SDR value for each catchment over the study areas was determined through an empirical function developed in central SiChuan province (Li et al., 1995) where the catchments are similar in topographic conditions to HeMingGuan and LiZiKou:

$$SDR = 0.46A_c^{-0.158} \tag{8}$$

where A_c is the area of the catchment (km^2).

Besides the use of a single value of SDR for the whole catchment, the neglected differences in soil characteristics, land use practices between experimental plots and the grid cells could also cause unpredictable bias in the simulated output. To account for various factors that are not included in the simulation, an adjustment coefficient was introduced to each catchment. Thus the sediment yield at the outlets can be calculated using the following equation:

$$SY_{outlet} = C \cdot SDR \cdot \sum SY_i \tag{9}$$

in which SY_{outlet} is the sediment yield (kg) at the outlet of catchment; C is an adjustment coefficient which can be determined through calibrating against observed sediment yields in the model development area.

4. Input data and parameter estimation

Parameters required by WetSpa Extension include "default parameters" that vary with land use type, soil type and/or slope
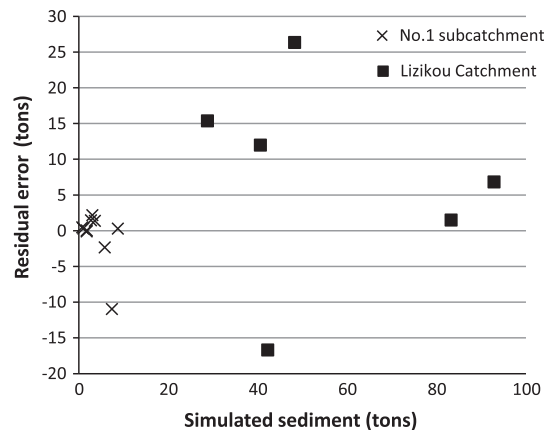

Fig. 8. Residual errors in simulating sediment yields for Sub-catchment No. 1 and LiZikou catchment.
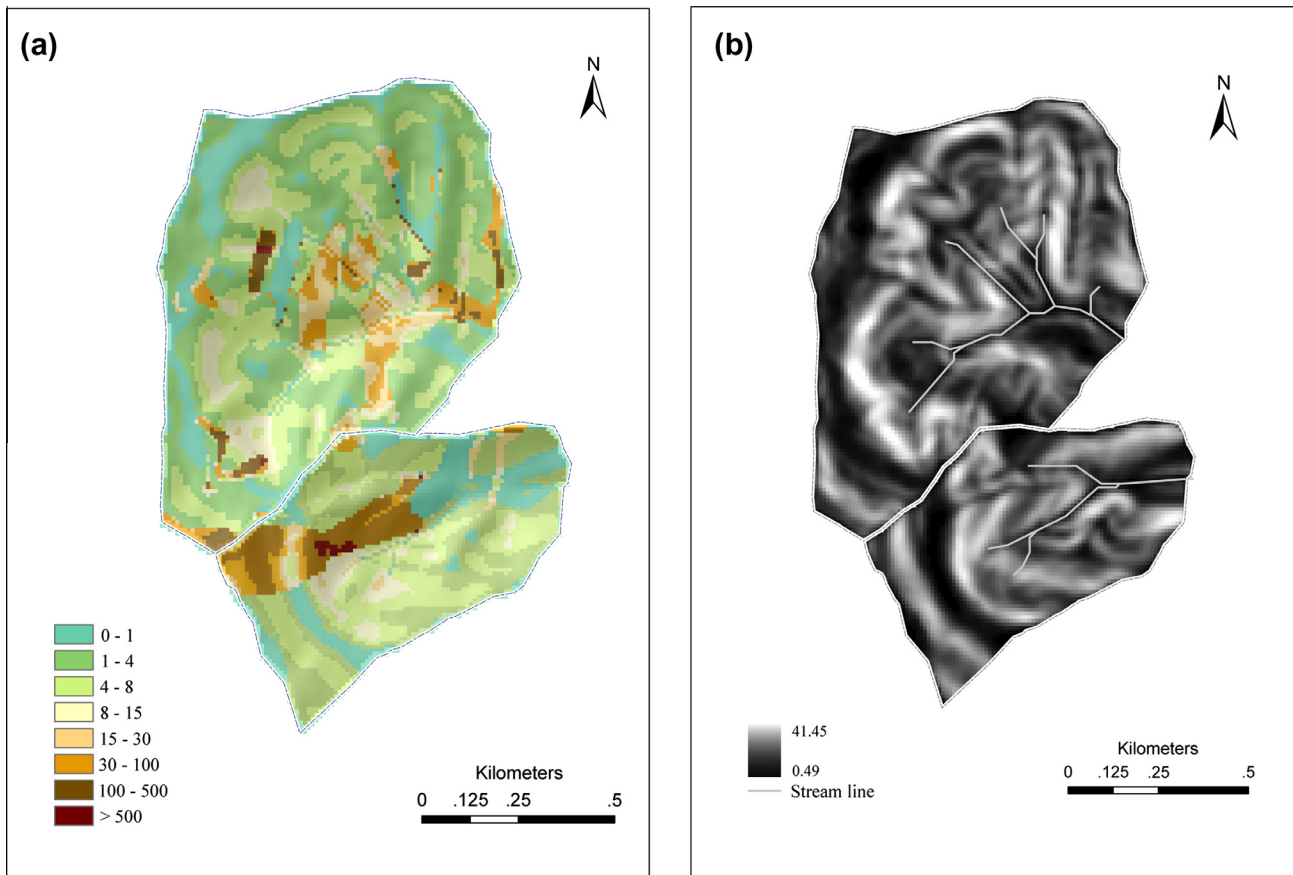
Fig. 9. The August 8th of 1998 storm event in HeMingGuan catchment (a) spatial distribution of simulated erosion rates (tons/km^2), (b) slope gradients (°).

gradient, and "global parameters" that remain constant over the watershed. In WetSpa Extension, lookup tables are provided with default values for all default parameters (Liu and De Smedt, 2004). We used default values in those lookup tables for each grid cell according to the local land use, soil, and/or slope gradient.

The empirical coefficients between water discharge and sediment yield under different land uses were derived through regression analysis. The land use types of the study area included wood land, crop land (tillage), terrace land, rice paddy, and residential areas. Since rice paddy was filled with water, we excluded it as well as residential areas (due to its limited extent) from areas of sediment source. Therefore we needed empirical functions for wood land, crop land and terrace land for simulating soil loss in the study area. The resultant regression relationships are shown in Fig. 5. The three functions are all in the form of $S = aR^b$, in which all "b"s are similar (close to 1), while coefficient "a"s differ substantially from each other: "a" for planted wood land is 0.0002, for terrace land is 0.0027, and for crop land is 0.0168. These considerable differences in the value of "a" reveal that, among the three land use types, crop land is most prone to erosion, and wood land is least. The input parameters to the model are summarized in Table 4.

5. Model calibration and validation

The coupled model was calibrated for the study areas using the most recent observed data series over the period from May 1st to October 31st of 2001 in Sub-catchment No. 2 of HeMingGuan catchment (Fig. 6). It is noted that the calibrated parameters were set up at the beginning date of the period and then run continually

throughout the entire period without changes. An optimal match between observed and simulated flow discharges was eventually achieved by adjusting the initial input values of the parameters. Without any further modifications, the calibrated parameter sets were then applied to Sub-catchment No. 2 over the same period of every year from 1993 to 2000. The effectiveness of model simulation was evaluated both graphically and statistically. Four types of statistical indices were used in assessing model performance, including the Nash–Sutcliffe efficiency (NSE) (Nash et al., 1970), Standard deviation ratio (RSR), Percent bias (PBIAS) and Coefficient of determination (R^2). NSE indicates how well the plot of observed versus simulated data fits the 1:1 line. NSE ranges from $-\infty$ to 1.0 (1 inclusive) with NSE = 1 being the optimal value. Values between 0.0 and 1.0 are generally viewed as acceptable levels of performance, whereas values <0.0 indicates that the mean observed value is a better predictor than the simulated value, which indicates unacceptable performance (Moriasi et al., 2007). RSR is one of the commonly used error index statistics and varies from the optimal value of 0. The lower RSR, the better the model performance is. Percent bias (PBIAS) measures the average tendency of the simulated data to be larger or smaller than their observed counterparts (Gupta et al., 1999). The optimal value of PBIAS is 0.0 with low-magnitude values indicating accurate model simulation. Positive values indicate model underestimation bias, and negative values indicate model overestimation bias (Gupta et al., 1999).

Fig. 7 and Table 5 show a mixed result of the observed and simulated hydrographs for Subcatchment No. 2. The model reproduced hydrograph reasonably well for 1993, 1994, 1996, 1998, 1999 and 2000, with NSE values greater than 0. However, the simulated and observed hydrograph was poorly fitted for 1995 and 1997. It is
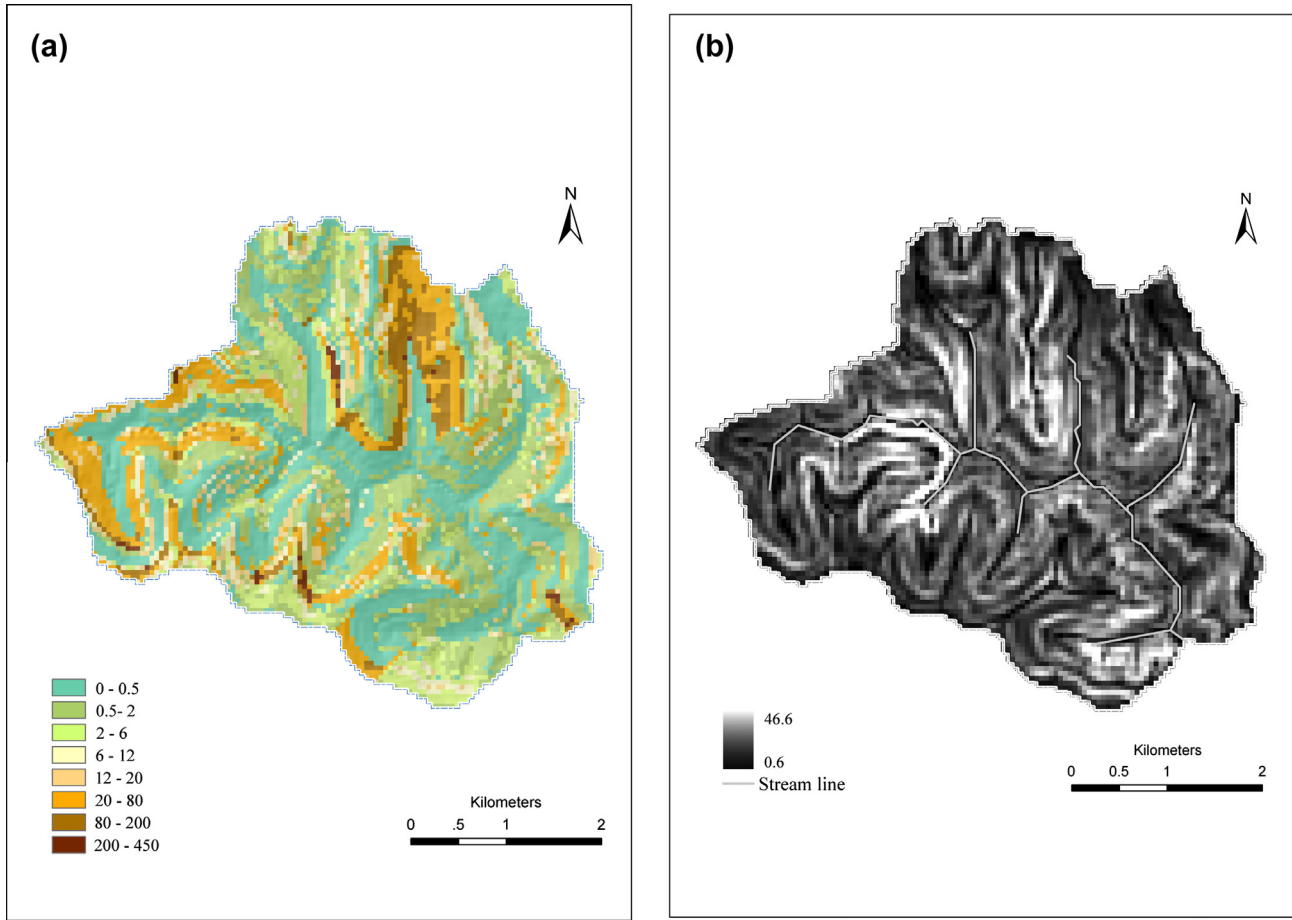
Fig. 10. The September 19–21 of 2004 storm event in LiZhiKou catchment. (a) Spatial distribution of simulated erosion rates (tons/km^2) and (b) slope gradients (°).
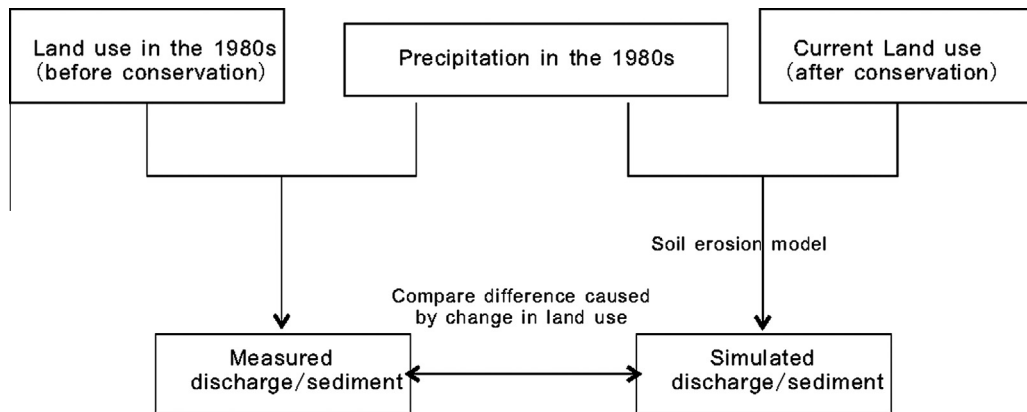

Fig. 11. Flow chart of the model application.

noted that flow discharges were very low for the both years. In addition, simulated peak flows were often delayed by 1 day from the observed ones. Further examinations showed that low peak discharges were usually overestimated while high peak discharges were underestimated, as shown in Fig. 7. The delayed time to peak flow and the underestimation of peak flow discharges by model simulation are probably caused by the uniform daily modeling time step in the present study. The WetSpa Extension requires variable time steps ranging from a few minutes within a storm to 1 day between storms (Liu, 1999; Liu et al., 2003). The poor simulation of time to peak flows and the overall underestimation of

peak flow discharges suggest that the model cannot be used in flood prediction with a uniform daily modeling time step in the area.

With the daily discharge data aggregated by week (Table 6), the model performance was dramatically improved, with an increase of NSE from 0.029 to 0.654 and a decrease of RSR from 0.942 to 0.119, respectively. The better performance can be explained by lumping the delayed peak flows through aggregation of daily discharges. A further increase in the aggregated time length from week to month only results in a slight improvement in model performance, with an increase of NSE value from 0.654 to 0.729. The
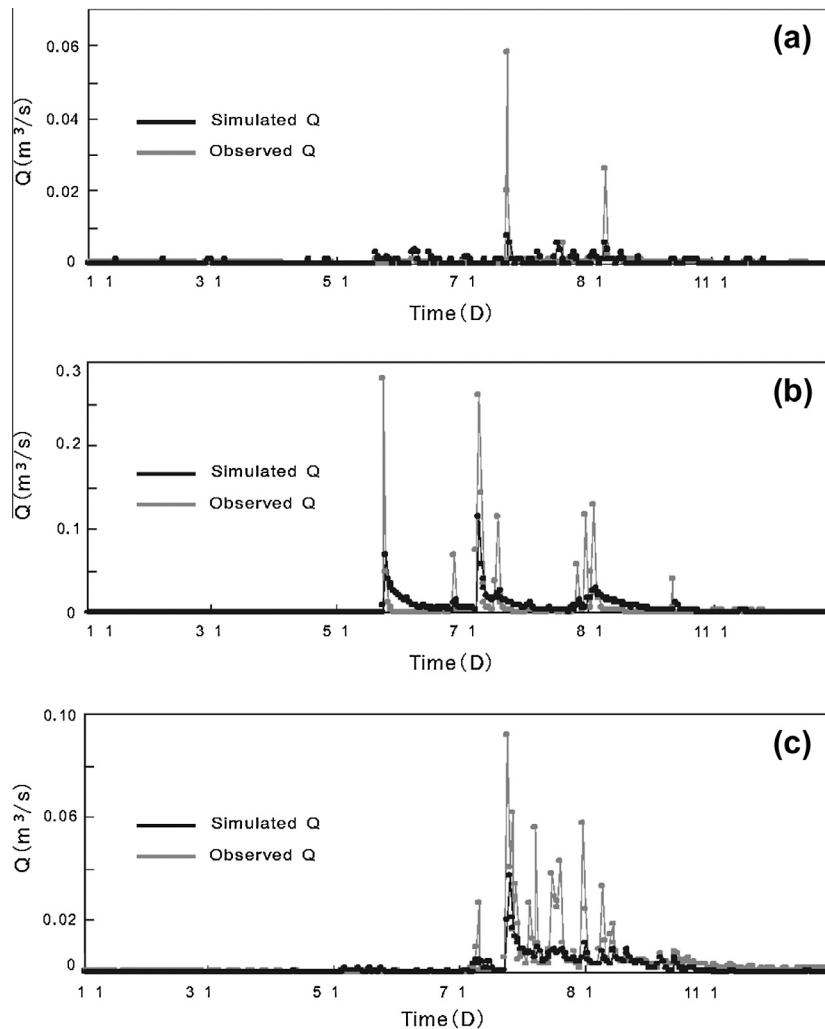
Fig. 12. Simulated sediment yields under current land use conditions vs. observed sediment yields over the period of 1986 through 1988 in Sub-catchment No. 2.

high values of NSE and R^2 and the low values of RSR and PBIAS of weekly and monthly flow discharge simulation shown in Table 6 suggest that WetSpa Extension is an effective tool in water resources management in the area.

The erosion component of the model was calibrated using the observed sediment yield in Sub-catchment No. 2 of the HeMing-Guan watershed as well. The calibrated parameter sets were then applied to Sub-catchment No. 1 and LiZiKou catchment without any modifications. It should be noted that due to the limited number of observed events in both Sub-catchment No. 1 and the LiZiKou catchment, we grouped them together for validation purpose. The Sub-catchment No. 1 has a much smaller size and yields relatively small volume of sediment while the LiZiKou catchment is a larger catchment and produces relatively large volume of sediment. Combining the two catchments allows us to examine how the model performs over a relatively wide range of sediment yields. Overall, the simulated sediment yields compared well with the observed ones (Table 7 and Fig. 8), with a NSE value of 0.88. Given the fact that the model was not recalibrated, we can conclude that the portability of the developed model is good when it is applied to the nearby and similar catchments.

To examine spatial distribution of soil loss in the study areas, we chose two relatively large storm events with a great range of erosion rates that could present enough spatial variability. The storm chosen for HeMingGuan catchment was the one on August 20th, 1998 with the event precipitation of 105.88 mm. The ob-served average erosion rate in No. 1 sub-catchment and that in No. 2 sub-catchment are 22.92 t/km^2 and 20.685 t/km^2, respectively. The storm chosen for Lizikou catchment occurred from 19th to 21st, 2004, during which the precipitation was 73.8 mm and the average erosion rate was 4.17 t/km^2. The simulated distribution of erosion rates for the two sub-catchments and Lizikou catchment is shown in Figs. 9a and 10a, respectively.

As reported in many other studies on spatially-distributed erosion modeling it is difficult to evaluate spatial pattern of erosion quantitatively when sediment data is sparse over the area of interested catchments (e.g., Takken et al., 1999; He and Walling, 2003; Merritt et al., 2003). In this paper we evaluate the validity of spatial variability of erosion rates through a visual comparison between erosion rate map and land use map as well as between erosion rate map and slope gradient map for each catchment. First, we compared the distribution of erosion rate (Figs. 9a and 10a) with the corresponding distribution of land use (Fig. 3), and found that distribution of erosion rates over space was mainly controlled by land use types. All the high erosion rates from 20 up to hundreds of tons per km^2 occurred in the areas of crop land, while all areas of wood land experienced very low erosion rates, mostly less than 10 t/km^2. Furthermore, we compared the distribution of erosion rates with corresponding distribution of slope gradient (Figs. 9b and 10b). Within the regions of the same land use, erosion rates showed a similar pattern as the corresponding slope gradient. The steeper the slope gradients, the higher the erosion rates were. Relatively,

Table 8
Comparison of erosion with and without landuse changes for storm events at No. 2 sub-catchment.

Year	Date	Erosion without landuse changes (measured) (tons)	Erosion with landuse changes (simulated) (tons)	Year	Date	Erosion without landuse changes (measured) (tons)	Erosion with landuse changes (simulated) (tons)
1985	6.27–28	115.7	2.3	1987	8.25–26	21.3	0.3
	7.1	168.7	0.1		8.30	159.2	0
	7.21	78.9	0		9.1–3	57.1	1.4
	8.7–10	318.2	0.2		10.11	41.2	0
	8.18–19	41	0	1988	7.8–10	13.6	0.1
	9.13–14	83.2	2.3		7.23–25	307.9	4.7
1986	7.23	61.6	0		7.27–28	13.4	0
	9.8–9	8.7	0		8.3–4	9.7	0
1987	5.23–26	287	12.0		8.7	62.2	0
	6.21–22	2.7	0		8.13–18	83.7	0
	6.26–27	56.2	0.7		8.29–30	41.3	0
	7.8–10	390.3	18.6		9.7	5.2	0
	7.16–18	20.5	1.5		9.11–12	6.5	0

high erosion rates were also found in areas nearby stream lines where a high volume of flow accumulated, especially in the HeMingGuan catchment in which crop lands are frequently located along the stream lines. These qualitative comparisons show that the simulation approach in this study is capable of producing realistic patterns of spatial variability of soil erosion rates, which reflects the combined effect of land uses and topographic features.

6. Model application

Given that the model simulates sediment yields reasonably well, as shown in Table 7 and Fig. 8, we apply the model to assess the effectiveness of land use changes for soil and water conservation purpose in reducing erosion. Land use changes were implemented in Sub-catchment No. 2 of HeMingGuan since early 1990s. Thus, the observed discharge and sediment records over the period of 1986 through 1988 represented the rainfall-runoff relation and erosion processes prior to land use changes. We can combine the precipitation series from 1986 to 1988 with the changed land uses to simulate discharges and sediment yields to examine the effect of landuse changes because in this way the major differences between these simulated values and the observed values would be caused by the differences in land uses (Fig. 11). In other words, the simulated values and observed values represented the ones with and without the implementation of soil conservation measures, respectively. The results shown in Fig. 12 indicate that the peak flows reduced significantly for all the 3 years with the implementation of soil and water conservation. We also found the sediment yields for storm events were reduced by one or two order(s) of magnitude (Table 8). The soil loss was reduced by an overall of 98.9%, ranging from 92.7% to 100%, which is, to a certain degree, a testimony of the effectiveness of the water and soil conservation practices implemented through land use changes.

7. Discussion and conclusions

Sedimentation is a serious concern in the Three-Gorge Reservoir and integrated small watershed management (ISWM) through land use changes and soil conservation practices is a fundamental solution to this concern. This paper presents a modeling approach to simulating soil erosion based on limited existing plot data in the small catchments of the TGR drainage area. Under the framework of a physically-based spatially-distributed hydrological model WetSpa Extension, empirical relationships between soil loss and runoff derived from experimental plots under different land use conditions were then incorporated to calculate soil erosion in grid cells. A topographic factor was also developed to account for impacts of topography on soil erosion. Finally a constant SDR is applied to calculate sediments transported to outlets from grid cells.

The hydrologic component of the model reproduces stream flow hydrographs reasonable well in most of the years, but it often does not simulate time to peak flows well and the peak flow rates are considerably underestimated. This is probably, to a great degree, caused by the large and uniform modeling time step. Besides, time-to-peak is affected by drainage network density, slope, channel roughness, and soil infiltration characteristics (Fiedler and Ramírez, 2000), and peak flow rates are typically affected by within-storm rainfall characteristics which are not well reflected by daily precipitation in the model. In the future, it is needed to examine the simulation with high resolution rainfall data and flow discharge data. The model performance is dramatically improved by aggregating daily discharges into weekly and monthly discharges. Thus, with a daily time step, the model is an effective tool for water resources planning and management, though not for flood prediction.

The erosion component of the model does not simulate detachment, transport and depositional processes, which would otherwise require much more input data. Instead, it simulates soil erosion rates at pixel level by incorporating the simple regression relation between discharge and sediment yield at plot level. Such field measurement plot data are available in many experimental watersheds in the TGR drainage area, which assures the model having a great potential to be applied in the region. Although the model does not simulate the sediment transport processes within the catchment, the simple sediment delivery ratio makes it possible to compute sediment yields exit from the catchment, which is especially important in the TGR drainage area. A comparison of simulated and observed sediment yields indicates that the model performance is satisfactory in soil loss simulation within the watershed.

There are issues, however, about utilizing the data from experimental plots to simulate soil erosion in the watershed. The main concern is that the erosion types occur in the plots may not represent all erosion types in a watershed (Mukundan et al., 2012). In our study, for example, soil erosion in the plots was produced by hillslope erosion, and all other types of erosion such as gully erosion and mass movements cannot be represented by the available plots data. It is acceptable in this study to neglect gully erosion because the study areas are fairly small and gully erosion is not a major erosion form there. Scale problem is another issue which is related to directly applying empirical relationships derived from plots to grid cells in the catchments. Ideally, the area of a grid cell should be same as that of the plots, so that the empirical relationship between runoff and soil loss from plots can seamlessly be transferred to grid cells. The plot size in our study is around

200 m². However, the areas of a grid in HeMingGuan and LiZiKou are both different from 200 m², which might have caused additional errors, especially for LiZiKou catchment where the area of a grid is over ten times of the plot. Further research could be conducted to study the sensitivity of simulated results to the difference between plot size and cell size.

It can be concluded that albeit the aforementioned problems, the modeling approach presented in this study is capable of predicting pixel soil erosion rates and catchment sediment yields as well as weekly and monthly streamflow discharges reasonably well. In the future, the issues discussed above need to be further explored and our ultimate goal is to make this modeling approach become an effective tool in assessing land use changes and soil conservation practices in the TGR drainage areas.

Acknowledgements

References

Arnold, J.G., Srinivasan, R., Muttiah, R.S., Williams, J.R., 1998. Large area hydrologic modeling and assessment Part I: model development. J. Am. Water Resour. Assoc. 34 (1), 73–89.

Band, L.E., 1986. Topographic partition of watersheds with digital elevation models. Water Resour. Res. 22, 15–24.

Band, L.E., 1993. Effect of land surface representation on forest water and carbon budgets. J. Hydrol. 150, 749–772.

Band, L.E., Hwang, T., Hales, T.C., 2011. Ecosystem processes at the watershed scale: mapping and modelling ecohydrological controls of landslides. Geomorphology 137, 159–167.

Batelaan, O., Wang, Z.M., De Smedt, F., 1996. An adaptive GIS toolbox for hydrological modeling. In: Kovar, K., Nachtnebel, H.P. (Eds.), Application of Geographical Information Systems in Hydrology and Water Resources, IAHS Publ. No. 235, pp. 3–9.

Carson, M.A., Kirkby, M.J., 1972. Hillslope Form and Process. Cambridge University Press, Cambridge.

De Roo, A.P.J., Wesseling, C.G., Ritsema, C.J., 1996. LISEM: a single-event physically based hydrological and soil erosion model for drainage basins: I. Theory, input and output. Hydrol. Process. 10, 1107–1117.

De Smedt, F., Liu, Y.B., Gebremeskel, S., 2000. Hydrological modeling on a catchment scale using GIS and remote sensed land use information. In: Brebbia, C.A. (Ed.), Risk Analyses II. WIT Press, Southampton, Boston, pp. 295–304.

Desmet, P.J.J., Govers, G., 1996. A GIS procedure for automatically calculating the USLE LS factor on topographically complex landscape units. J. Soil Water Conserv. 51 (5), 427–433.

Fiedler, F.R., Ramírez, J.A., 2000. A numerical method for hydrodynamic modeling of overland flow. Int. J. Numer. Methods Fluids 32 (2), 219–239.

Foster, G.R., Wischmeier, W.H., 1974. Evaluation irregular slopes for soil prediction. Trans ASAE 17 (2), 305–309.

Gupta, H.V., Sorooshian, S., Yapo, P.O., 1999. Status of automatic calibration for hydrologic models: comparison with multilevel expert calibration. J. Hydrol. Eng. 4 (2), 135–143.

He, Q., Walling, D.E., 2003. Testing distributed soil erosion and sediment delivery models using 137Cs measurements. Hydrol. Process. 17, 901–916.

HEC, 1995. Application of Methods and Models for Prediction of Land Surface Erosion and Yield. Training Documents No. 36 (March).

Hoyos, N., 2005. Spatial modeling of soil erosion potential in a tropical watershed of the Colombian Andes. Catena 63, 85–108.

Hu, B.Q., Yang, Z.S., Wang, H.J., Sun, X.X., Bi, N.S., 2009. Sedimentation in the Three Gorges Dam and its impact on the sediment flux from the Changjiang (Yangtze River), China. Hydrol. Earth Syst. Sci. Discuss. 6, 5177–5204.

International Soil Conservation Organization (ISCO), 2002. 12th ISCO Congress Conference, May 26–31, Beijing, China.

Kirkby, M.J., Chorley, R.J., 1967. Throughflow, overland flow, and erosion. Int. Assoc. Sci. Hydrol. Bull. 12 (3), 5–21.

Li, Q.Y., Sun, H.C., Jiang, S.Q., 1995. Fractal character and statistical model of sediment delivery of small watersheds in hilly area of purple soils. J. Yangtze River Sci. Res. Inst. 12 (2), 30–35.

Liao, C.Y., 2010. Soil and water conservation in Yangtze River Basin during past 60 years: review and perspective. Yangtze River 41, 2–6 (in Chinese).

Liu, B.Y., Nearing, M.A., Risse, L.M., 1994. Slope gradient effects on soil loss for steep slopes. Trans. ASAE 37, 1835–1840.

Liu, B.Y., Nearing, M.A., Shi, P.J., Jia, Z.W., 2000. Slope length effects on soil loss for steep slopes. Soil Sci. Soc. Am. J. 64, 1759–1763.

Liu, Y.B., 1999. A GIS-based Spatially Distributed Hydrological Modelling of the Barebeek Catchment. MSc. Thesis. Inter-University Programme in Water Resources Engineering, Katholieke Universiteit Leuven and Vrije Universiteit Brussel, Belgium.

Liu, Y.B., De Smedt, F., 2004. WetSpa Extension, Documentation and User Manual. Department of Hydrology and Hydraulic Engineering, Vrije Universiteit Brussel, Brussels, Belgium.

Liu, Y.B., Gebremeskel, S., De Smedt, F., Pfister, L., 2002. Flood prediction with the WetSpa model on catchment scale. In: Wu, B., Wang, Z., Wang, G., Huang, G., Fang, H., Huang, J. (Eds.), Flood Defense. Science Press, New York Ltd., NY, pp. 499–507.

Liu, Y.B., Gebremeskel, De Smedt, F., Hoffmann, L., Pfister, L., 2003. A diffusive transport approach for flow routing in GIS-based flood modeling. J. Hydrol. 283, 91–106.

Lu, X.X., Higgitt, D.L., 2000. Estimating erosion rates on sloping agricultural land in the Yangtze Three Gorges, China, from caesium-137 measurements. Catena 39, 33–51.

Lu, X.X., Higgitt, D.L., 2001. Sediment delivery to the Three Gorges: 2: local response. Geomorphology 47, 157–169.

Mahmood, K., 1987. Reservoir Sedimentation: IMPACT, Extent and Mitigation, World Bank Technical Paper No. 71, Washington, DC, USA.

McCully, P., 1996. Silenced Rivers: The Ecology and Politics of Large Dams. Zed Books, London, 416pp.

Merritt, W.S., Letcher, R.A., Jakeman, A.J., 2003. A review of erosion and sediment transport models. Environ. Model. Softw. 18, 761–799.

Moore, I.D., Burch, G.J., 1986a. Modelling erosion and deposition: topographic effects. Truns. Am. Soc: Agric. Enqrx. 29 (1624–1630), 1640.

Moore, I.D., Burch, G.J., 1986b. Physical basis of the length–slope factor in the universal soil loss equation. Soil Sci. Soc. Am. J. 50, 1294–1298.

Moore, I.D., Nieber, J.L., 1989. Landscape assessment of soil erosion and nonpoint source pollution. J. Minnesota Acad. Sci. 55 (1), 18–25.

Morgan, R.P.C., Quinton, J.N., Smith, R.E., Govers, G., Poesen, J.W.A., Auerswald, K., Chisci, G., Torri, D., Styczen, M.E., 1998. The European soil erosion model (EUROSEM): a dynamic approach for predicting sediment transport from fields and small catchments. Earth Surf. Proc. Land. 23, 527–544.

Moriasi, D.N., Arnold, J.G., Van Liew, M.W., 2007. Model evaluation guidelines for systematic quantification of accuracy in watershed simulations. Trans. ASABE 50 (3), 885–900.

Mukundan, R., Walling, D.E., Gellis, A., Slattery, M., Radcliffe, D., 2012. Sediment source fingerprinting: transforming from a research tool to a management tool. J. Am. Water Resour. Assoc. 48, 1241–1257.

Nash, J.E., Sutcliffe, J.V., 1970. River flow forecasting through conceptual models: Part 1. A discussion of principles. J. Hydrol. 10 (3), 282–290.

Nearing, M.A., Foster, G.R., Lane, L.J., Finkner, S.C., 1989. A process-based soil erosion model for USDA-water erosion prediction project technology. Trans. ASAE 32 (5), 1587–1593.

Qin, C., Zhu, A., Pei, T., Li, B., Zhou, C., Yang, L., 2007. An adaptive approach to selecting a flow-partition exponent for a multiple-flow-direction algorithm. Int. J. Geograph. Inf. Sci. 21 (4), 443–458.

Renard, K.G., Foster, G.A., Weesies, D.A., Mccool, D.K., Yoder, D.C., 1997. Predicting Soil Erosion by Water: A Guide to Conservation Planning with the Revised Universal Soil Loss Equation (RUSLE) Agriculture Handbook No. 703. USDA, Washington, DC.

Shi, Z., Ai, L., Fang, N., Zhu, H., 2012. Modeling the impacts of integrated small watershed management on soil erosion and sediment delivery: a case study in the Three Gorges Area, China. J. Hydrol. 438–439, 156–157.

Takken, I., Beuselinck, L., Nachtergaele, J., Govers, G., Poesen, J., Degraer., 1999. Spatial evaluation of a physically-based distributed erosion model (LISEM). Catena 37, 431–447.

Wang, Z.M., Batelaan, O., De Smedt, F., 1997. A distributed model for water and energy transfer between soil, plants and atmosphere (WetSpa). Phys. Chem. Earth 21 (3), 189–193.

Williams, J.R., 1975. Sediment-yield prediction with universal equation using runoff energy factor. In: Present and Prospective Technology for Predicting Sediment Yield and Sources: Proceedings of the Sediment Yield Workshop, USDA Sediment Lab., Oxford, MS, November 28–30, 1972, ARS-S-40.

Wischmeier, W.H., Smith, D.D., 1978. Predicting Soil Erosion Losses: A Guide to Conservation Planning. USDA Agricultural Handbook. No. 537. US Government Print Office, Washington, DC.

Zhang, K.L., Shu, A.P., Xu, X.L., Yang, Q.K., Yu, B., 2008. Soil erodibility and its estimation for agricultural soils in China. J. Arid Environ. 72, 1002–1011.